Original Research Article

Chemical constituents of *Combretum dolichopetalum*: Characterization, antitrypanosomal activities and molecular docking studies

Charles O Nnadi[1]*, Raphael Onuku[1], Thecla O Ayoka[2], Ndidiamaka H Okorie[3], Ngozi J Nwodo[1]

[1]Department of Pharmaceutical and Medicinal Chemistry, Faculty of Pharmaceutical Sciences, [2]Department of Science Laboratory Technology (Biochemistry Unit), Faculty of Physical Science, University of Nigeria, Nsukka 410001, [3]Department of Pharmaceutical and Medicinal Chemistry, Faculty of Pharmaceutical Sciences, Enugu State University of Science and Technology, Enugu, Nigeria

*For correspondence: **Email:** charles.nnadi@unn.edu.ng; **Tel:** +234-8064947734

Abstract

Purpose: To evaluate the in vitro activities of a gallic acid ester and two apigenin flavone glucoside constituents of Combretum dolichopetalum against Trypanosoma brucei brucei s427 (Tbs427) and Trypanosoma congolense IL3000 (Tc-IL3000), and their interactions with a lysosomal papain-like cysteine protease (CP) enzyme in silico.
Methods: Anti-trypanosomal activity-guided separation of ethyl acetate fraction using column chromatographic (CC) technique and purification of the CC sub-fractions with semi-preparative HPLC yielded three (1-3) compounds. The structures were characterized based on nuclear magnetic resonance (NMR) spectroscopic analyses and tested for activities against Tbs427 and Tc-IL3000. All the compounds were subjected to molecular docking studies for the inhibition of trypanosomal cathepsin B (TbCatB) CP.
Results: An ester (1), a butyl gallate, and two positional isomeric apigenin flavone glucosides (2, 3) were identified. The compounds 2 (vitexin) and 3 (isovitexin) showed low in vitro IC_{50} against the tested parasites. However, 2 (IC_{50}, 25 µM) was more potent than 3 (IC_{50}, 68 µM) against Tbs427 while both were equipotent (IC_{50} = 2, 11.5 µM and 3, 10.8 µM) against Tc-IL3000. Compound 1 (butyl gallate) showed higher activity against Tc-IL3000 (IC_{50} = 0.80 µM) than to Tbs427 (IC_{50}, 2.72 µM). The molecular docking study showed that all the compounds had minimum binding energies with a higher affinity towards the active pocket of TbCatB compared to the controls and native inhibitor (CA074).
Conclusion: The relatively high in vitro activities and their strong affinity for TbCatB support the need for further optimization of the compounds towards lead identification against animal trypanosomiasis.

Keywords: Cathepsin B, Combretum dolichopetalum, Docking, Flavone, Gallate, Afican trypanosomasis

----

INTRODUCTION

Animal African trypanosomiasis (AAT), caused by *Trypanosoma brucei* and *T. congolense*, is a major constraint in animal production, food safety and security in sub-Saharan Africa [1]. The debilitating effects on livestock production in sub-Saharan Africa are enormous and this has resulted in the death of millions of livestock [2]. Vaccination, chemotherapy, vector and parasite control methods of eradicating AAT have been advocated in Africa [3]. However, vector and parasite control methods have not yielded the desired results. Antigenic variation in trypanosomes has hampered efforts towards developments of vaccines [4]. Drug resistance is on the increase because no new drugs have been developed in the past decades [5]. More importantly, majority of the drugs clinically in use today were developed without adequate knowledge of the biochemical pathways [6]. Therefore, there is still a need, to develop new and highly selective molecules with an understanding of their effects on biochemical pathways for the control of animal trypanosomiasis. In this study, many natural products have shown potential as lead compounds [7,8].

Combretum dolichopetalum (Family Combretaceae), known for its long-term use in ethnomedicine, is a wild tropical medicinal plant widely distributed in Nigeria [9]. Based on the ethnomedicinal data gathered from local users, the methanol extract and different solvent fractions of this plant have been investigated for their medicinal uses in some protozoal and microbial infections. The preliminary results, in addition to the previously reported anti-trypanosomal activities of the plant necessitated this study [10,11]. As part of ongoing research to discover medicinal plant-based natural products (NPs), three compounds were isolated from *C. dolichopetalum* and tested for anti-trypanosomal activities, thereby opening up new knowledge about Combretaceae.

To understand the interaction of these compounds with a specific target in the parasite, an *in silico* docking study is imperative [7]. This method is an evolving complement to *in vitro* studies due to time, cost and ethical issues. Trypanosomal cathepsin B (TbCatB), a lysosomal cysteine protease (CP) of the papain superfamily, is widely expressed in both *T. brucei* and *T. congolense* and is produced by the parasites during infection of the host [12]. It is implicated in the progression of both human and animal trypanosomiasis. Cathepsin B is a vital enzyme in the biochemical pathway of trypanosomatids and represents a promising drug target for exploring novel chemotherapy against AAT due to its role in host protein degradation [13]. It has been reported that the knockdown of CatB in *T. brucei*-infected mice cured the infection by clearing the parasites from the bloodstream of the infected mice thereby qualifying CatB as a chemotherapeutic target [14]. Several CP inhibitors targeting CatB have further demonstrated the potential of CatB as a prime target for the development of new and selective anti-trypanosomal molecules for AAT [14]. In the present study, the isolation, characterization and bioactivity of an ester and two known apigenin flavone glucosides, as well as their interaction with CatB CP expressed in both *T. brucei* and *T. congolense* are reported.

This study is a step towards identifying potent natural product-inspired constituents of *C. dolichopetalum* by understanding interactions with important biochemical pathways in the parasite.

EXPERIMENTAL

General procedures

The NMR spectra were measured on DD2 600 MHz spectrometers (Agilent Technologies, CA). Samples were prepared in deuterated methanol (CD$_3$OD). The spectra were respectively referenced to the CD$_3$OD signals of a proton (3.31 ppm) and ^{13}Carbon (49.0 ppm) for solvent residual peaks using MestReNova version 11 (Chemistry Software Solutions, CA). The ^{1}H NMR data are reported showing the chemical shift values, δ (ppm), integral size, coupling constant(s), *J* (Hz) and multiplicity while the ^{13}Carbon NMR data reported as only the chemical shifts, σ (ppm). Compounds were purified using a complete HPLC system (Jasco, Germany), equipped with DAD MD 2018 plus, PU-2087 plus pump, autosampler AS 2055 plus, column thermostat CO 2060 plus, LC Net II ADC Chromatography Data Solutions. Silica gel 60 (0.060 - 0.200 mm; Merck KGaA GmbH, DE) was used for CC separation. Thin-layer chromatography (TLC) was performed using optimized mobile phase systems with silica gel 60 F$_{254}$ plates (Merck KGaA GmbH, Germany). Thin-layer chromatography (TLC) was used to monitor the collected CC fractions, and bands were viewed by spraying silica gel plates (set to 105 ºC) with anisaldehyde detecting reagent.

Plant material

The fresh leaves of *C. dolichopetalum* were collected in October 2018 with the help of a

botanist from a forest in Nsukka (N 7 43' 50", E 8 32' 10"), Nigeria. The plant was authenticated by Alfred Ozioko, a taxonomist at the International Center for Ethnomedicine and Drug Development (InterCEDD), Nigeria. A voucher (no. ICEDD110c) was stored at the herbarium of the Centre for future reference. The plant name was further confirmed at https://www.theplantlist.org at the time of collection.

Extraction and solvent partitioning

The aerial part of the plant was dried under shade for 14 days and pulverized into coarse powder (1 mm size). The powdered dry sample (1 kg) was extracted by cold maceration with 95 %v/v methanol at room temperature for 48 h, furnishing 85 g of a crude methanol extract after evaporation of solvent *in vacuo* at 40 ºC. The extract (80 g) was re-dissolved in 500 mL 10 %v/v methanol and successively partitioned in equal volumes *n*-hexane, ethyl acetate (EtOAc), *n*-butanol (n-But) and water to 1 L. This yielded *n*-hexane fraction (1.5 g), ethyl acetate fraction (9.8 g), *n*-butanol fraction (2.4 g) and water fraction (9.1 g) after evaporation to dryness.

Column chromatographic separation

The EtOAc fraction (5 g) was chromatographed on a column of silica gel and was eluted with mobile gradient of EtOAc-methanol mixture each gradient volume acidified with 5 mL formic acid. The mobile phase solvent was prepared as follows: 1.5 litres each of 100 % EtOAc, 9.9:0.1, 9.5:0.5 and 9.0:1.0 of EtOAc-MeOH. The eluates (in individual 20 mL tubes) were collected at a predetermined flow rate of 1 mL/min and analyzed by TLC to afford five fractions when combined as follows: Tubes 56 - 80 (Fraction 1, 0.4 g), tubes 84 - 107 (Fraction 2, 0.58 g), tubes 111-171 (Fraction 3, 1.10 g), tubes 178 - 208 (Fraction 4, 0.80 g) and tubes 210 - 255 (Fraction 5, 0.25 g).

Chromatographic purification of the active fractions

Fractions 3 and 4, obtained from the CC separation were further purified using semi-preparative HPLC. Separations were performed on a C-18 RP Reprosil 100 column (250 × 20 mm, 5 μm) using H_2O and MeOH gradient as the mobile phase, with 10 mL/min flow rate and 40 ºC column temperature. The sample was injected at a 1000 μL loop. The optimized mobile phase consisted of H_2O and MeOH in gradient conditions consisting: 60 to 30 % of H_2O for 5 min, 30 to 20 % H_2O for 5 min, 20 to 10 % of H_2O

for 5 min, 10 to 0 % H_2O for 5 min and 0 % H_2O for 5 min and followed by another 5 min to stabilize the HPLC system to the initial conditions. After repeated injections, fraction 3 (500 mg) yielded **1** (5.2 mg) while fraction 4 (400 mg) furnished **2** (9.1 mg) and **3** (5.8 mg) after repeated injections. Both fractions were prepared in a 10 mg/mL solution using the initial HPLC mobile phase solvent (40 % MeOH) for the isolation of compounds **1**-**3**.

In vitro biological activity assay

In vitro assays for the biological activity of the extract, fractions and isolated compounds against *Tb*s427 and *Tc*-IL3000 were performed using a resazurin-based assay protocol [3,15] using pentamidine and diminazene aceturate as standards. Serial dilutions of the extract/fractions and the compounds were prepared in 100 μL growth media from the stock solution of concentration of 100 μg/mL and 100 μM respectively. The samples were incubated for 48 h at 37 ºC (*Tb*s427) and 32 ºC (*Tc*-IL3000) in a 5 % CO_2 atmosphere. The IC_{50} values were obtained from non-linear regression equation for a sigmoidal dose-response curve.

In silico studies

Preparation of TbCatB structure

The 3D TbCatB and its co-crystallized inhibitor, CA074 (PDB ID: 3HHI, resolution 1.60 Å) was extracted from https://www.rcsb.org/ [16], and it was prepared in a Discovery Studio Visualizer (DSV) v17.2.0 (http://accelrys.com/downloads/updates/discovery-studio/dstudio2017r2/) before molecular docking. The crystallographic water molecules and other bound heteroatoms were removed for optimization. The protein was energy minimized using the methods of steepest descent (10^2 steps), and conjugate gradient, 10^1 steps, (sizes 0.02 Å) of the UCSF Chimera. Validation of the docking protocol and interacting residues between CA074 and the receptors were also performed [7].

Preparation of datasets

The 2D structures of 1-**3** as well as reference compounds (diminazene and pentamidine) were built with Marvin Sketch software and converted from .mol to .pdb file. The ligands were energy minimized using the MMFF94x force field. The PyRx-Python prescription 0.8 (200 steps) was adopted for the conjugate gradients optimization [7,17].

Molecular docking with AutoDock4.2

The docking algorithms of AutoDock Tools 1.5.6 (ADT) was used in the molecular docking. The protein structure and ligands were converted into (.pdbqt). The assignment of the torsions to the ligands was automatically executed using the Python scripts of the ADT and the customized python scripts. The native ligand was first re-docked into the TbCatB receptors for protocol validation after which compounds **1-3** and reference compounds were docked into the TbCatB receptors using the parameters obtained in the native ligand re-docking. The protein and the ligands were loaded into ADT with a grid box of 0.375 Å points spacing for the docking simulations [18]. The Lamarckian Genetic Search Algorithm was adopted as previously described [7]. The potential grid maps were executed using AutoGrid module with 250 hybrid GA-LS runs, ≤ 2.5 million energy evaluations and 0.27 million generations. A root mean square deviation of 2.0 Å was set to group the clusters. The visualization of the protein-ligand complex interaction patterns was performed using DSV.

RESULTS

Phytochemicals

The purification of the EtOAc fraction by semi-preparative HPLC yielded butyl gallate (**1**), in addition to two apigenin flavones glucoside, vitexin (**2**) and its positional isomer, isovitexin (**3**) [19] as shown in Figure 1. The compounds were identified from the ^1H and ^{13}C NMR spectra data, including 2D NMR experiments, which were also used to assign ^1H and ^{13}C chemical shifts of **1**. Butyl gallate (**1**) was isolated as a white amorphous solid; ^1H NMR (600 MHz, CD$_3$OD): δ 0.99 (t, *J* = 7.4 Hz, 3H), 1.50 (heptet, *J* = 8.0, 2H), 1.73 (pentet, *J* = 7.7, 2H), 4.24 (t, *J* = 6.5 Hz, 1H), 7.04 (s, 2H). ^{13}C NMR (150 MHz, CD$_3$OD): δ 168.6, 146.5, 146.5, 139.8, 121.7,
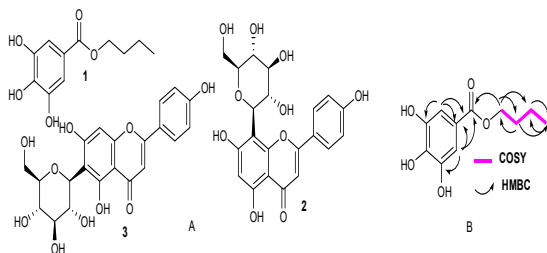
110.0, 110.0, 65.5, 32.0, 20.4, 14.1. MP: 112 - 115 ºC; MOL. FORMULA $C_{11}H_{14}O_5$; UV/VIS: ΛMAX = 220 NM; TR 6.933 MIN; ^1H NMR (CD$_3$OD, 600 MHZ) AND ^{13}C NMR (150 MHZ). Anti-trypanosomal activity

The *in vitro* activities profile of tested substances against *Tb*s427 and *Tc*-IL3000 are presented in Table 1. The methanol extract showed significant *in vitro* activity against *Tb*s427 (2.80 µg/mL) and *Tc*-IL3000 (2.01 µg/mL). It is imperative to note that biological activity-guided isolation protocol was adopted in this study. The fractionation of the extract and assay of the fractions showed that only the n-But and EtOAc soluble showed significant *in vitro* activities. Subsequent purification of the EtOAc fraction yielded three known compounds among which **1** showed the highest activity against both *Tb*s427 (2.72 µM) and *Tc*-IL300 (0.80 µM) strains. The comparatively high activities observed in the EtOAc fraction and its CC fractions 3 and 4 necessitated their further purification which resulted in isolation of **1**-**3**.

Table 1: *In vitro* antitrypanosomal activities of *C. dolichopetalum*

Sample tested	*Tb*s427 (IC$_{50}$)	*Tc*-IL3000 (IC$_{50}$)
Extract (µg/mL)	2.80±0.11	2.01±0.02
n-But fraction (µg/mL)	40.18±1.10	68.91±2.2
EtOAc fraction (µg/mL)	5.54±0.80	1.96±0.04
Fraction 3 (µg/mL)	11.80±0.12	1.00±0.20
Fraction 4 (µg/mL)	4.34±0.80	28.90±1.15
1 (µM)	2.72±0.05	0.80±0.03
2 (µM)	25.50±1.02	11.51±0.90
3 (µM)	68.22±2.25	10.58±0.77
Pentamidine (µM)	0.003±0.001	0.505±0.020
Diminazene (µM)	0.078±0.009	0.010±0.002

IC$_{50}$ is mean of (n = 3) independent determinations, expressed as mean IC$_{50}$ ± SD, aqueous and hexane soluble as well as EtOAc fractions 1, 2 and 5 showed IC$_{50}$ > 100 µg/mL

AutoDock 4.2 docking and scoring

AutoDock 4.2 software with the force field-based scoring function was employed for the virtual screening of the five ligands. A grid box points 52 x 50 x 46 with 0.375 Å spacing centered on the mass center of 5.356 x 1.505 x 43.722 which reproduced the pose of CA074, RMSD 0.98 Å was adopted in docking the 5 compounds. The binding free energy (E$_b$) and inhibition constant (K$_i$) of native ligand, **1-3** as well as controls are shown in Table 2. The result showed that **1** and **2** had E$_b$ close to both CA074 and reference diminazene.

Figure 1: (A) Compounds isolated from *C. Dolichopetalum*; **(B)** Key HMBC and COSY correlations of **1**

Table 2: Predicted binding energy and inhibition constant of **1-3**

Dataset	E_b (kcal/mol)	K_i (µM)
CA074	-5.72	64.45
1	-5.30	130.10
2	-5.81	55.21
3	-4.51	492.05
Diminazene	-5.64	73.84
Pentamidine	-3.81	1620.00

Docking validation

The docking validation showed some major interactions between TbCatB and CA074. The oxygen atom of the inhibitor formed H-bonds with N of Gln116 and Cys122. An interaction (H-bond) was formed between the terminal O-atom of CA074 and N atoms of His194 and His281. There were also electrostatic interactions between the terminal oxygen and Trp304. Important hydrophobic interactions were observed between the Gly120 and Pro167 and a C-atom of the ligand respectively In the re-docked protocol with CA074 the H-bond with Gln116 and the hydrophobic interaction with Gly120 and Pro167 were accurately replicated. Besides, the carbon atom of CA074 also formed hydrophobic interactions with Ala283 of the target.

Binding poses

The results of the binding poses of **1-3** (Figure 2, Figure 3 and Figure 4) showed biochemically interesting binding modes. Compound **1** interacted with Gly281, Cys122, Gln116, His195 and His282 (Figure 2) to form H- and hydrophobic bonds. Interaction with Cys122, Gly281 and Gln116 residues resulted in four H-bonds: two H-bonds between the -COOH group of Gly281 and H atoms of **1,** and between -NH groups of Cys122 and Gln116 and an O atom of **1**. The His195 and His282 formed a hydrophobic bond with **1**. However, there was a hydrophobic bond formation existing between the cyclic ring of **1** and the -SH group of Cys122. Compound **2** interacted with Asn163, Cys122, Gly281, His282, His194, His195, Cys119 and Cys205. Bonding between **2** and TbCatB was stabilized by seven H-bonds between the compound and the Asn163, Cys122, Gly281, His282, His194, and His195 residues.

Compound **2** utilized virtually all amino acid residues in its interaction with TbCatB protease compared with controls and CA074 (Figure 3). Compound **3** interacted with Cys122, His282, Gly281, Asn163, Gln116, Ser117, Ala118 and Gly164 (Figure 4). The following residues made

hydrogen bond interactions with the compound: Cys122, Gly281, His282 and Asn163.
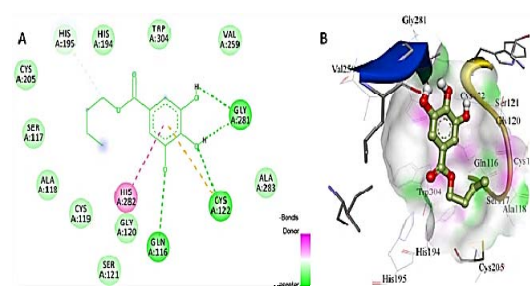

Figure 2: 2D representation of the interactions (A) and theoretical binding pose (B) of **1** and important TbCatB protease residues. The protein residues and the ligands are shown in line and in ball and stick formats respectively. Ligand atoms are coloured: gray = C, red = O, blue = N and white = H. The background represents the molecular surface of the protein according to DSV representation
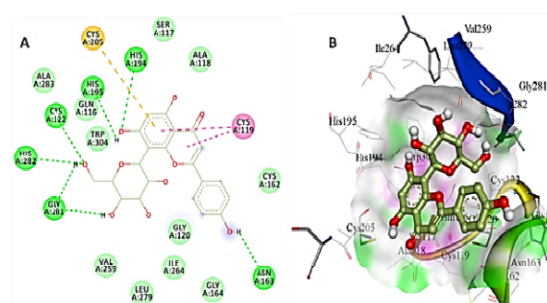

Figure 3: 2D representation of the interactions (A) and theoretical binding pose (B) of **2** and important TbCatB protease residues. The protein residues and the ligands are shown in line, and in ball and stick formats respectively. Ligand atoms are coloured: gray = C, red = O, blue = N and white = H. The background represents the molecular surface of the protein according to DSV representation
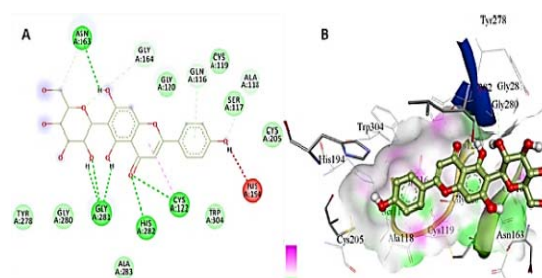

Figure 4: 2D representation of the interactions (A) and theoretical binding pose (B) of **3** and important TbCatB protease residues. The protein residues and the ligands are shown in line and in ball and stick formats respectively. Ligand atoms are coloured: gray = C, red = O, blue = N and white = H. The background represents the molecular surface of the protein according to DSV representation

DISCUSSION

The ^{1}H NMR of **1** revealed a signal corresponding to aromatic protons at δ_H 7.04 (*s*, H-2/6) that is typical of protons of a galloyl moiety. The presence of a single signal downfield δ_H 4.24 (*t*, 6.5 Hz) suggested the presence of an O-C-H group which was confirmed by the HSQC correlations. The combination of 1D and 2D NMR spectra of **1** revealed the presence of eleven signals corresponding to five non-hydrogenated carbons, including one carbonyl group at δ 168.6 (C-1'), two methines (CH); aromatic signals at δ 110.0, three methylene (CH$_2$) carbons including one linked to oxygen atom at δ_C 65.5/δ_H 4.24 and one methyl (CH$_3$) carbon at δ 14.1, leading to a molecular formula of $C_{11}H_{14}O_5$. The heteronuclear long-range couplings ($^3J_{HC}$) of carbon atom δ 168.6 (C-1') with H-2 (δ_H 7.04), H-6 (δ_H 7.04) and H-2' (δ_H 4.24) was used to confirm the position of a carbonyl functional group linked to C-1'. The presence of a methyl group bonded to an sp^3 methylene carbon was recognized by a triplet signal at δ_H 0.99 (*t*, *J* = 7.9 Hz, H-5'), the multiplet (heptet) at δ_H 1.50 (*h*, *J* = 8.0 Hz, H-4'), the multiplet (pentet) at δ_H 1.73 (*p*, *J* = 7.7 Hz, H-3') and a triplet signal at δ_H 4.24 (*t*, *J* = 6.5 Hz, H-2') characterizing an O-CH$_2$-CH$_2$-CH$_2$-CH$_3$ moiety corresponding to CH$_2$-2', CH$_2$-3', CH$_2$-4' and CH$_3$-5' respectively, typical of aliphatic chains [20]. This moiety was further confirmed by long-range correlations revealed using the HMBC and COSY spectra through correlations as illustrated in Figure 1B. The data described suggested a galloyl moiety linked to a butyl unit. These NMR spectral data were in full agreement with butyl gallate previously isolated from *Pelargonium reniforme* [21]. Other flavonoids have been reported elsewhere [19]. However, all the compounds are reported for the first from *C. dolichopetalum*.

This study investigated for the first time the activity of *C. dolichopetalum* and its constituents against the AAT-causing parasite. Previous studies had shown the trypanocidal potential of *Combretum* species but did not identify the phytochemical constituents responsible [10,11]. The anti-*Tb*s427 and *Tc*-Il3000 activities of the isolated compounds ranged from 2.72 – 68.22 µM and 0.80 – 11.51 µM respectively. The most active of the three compounds identified was **1** which was never isolated or tested for antitrypanosomal activity. The other two compounds showed low activities against *Tb*s427 and moderate activities against *Tc*-IL3000. These results necessitated an *in silico* molecular docking study which is fundamental for further development of these compounds for use in the chemotherapy of AAT.

Drug discovery with a clear understanding of the different biochemical pathways in the target parasite is important to reduce the off-target effects of molecules [7]. *T. brucei* CatB is well expressed in both *T. brucei* and *T. congolense* and contributes significantly to the pathogenesis of AAT. This study further provides *in silico* evidence of possible interaction of **1-3** with a CP enzyme (CatB) that could be responsible for the biological activities recorded in the *in vitro* studies. Docking screening of the isolated compounds against the TbCatB target site revealed that **2** exhibits better binding potential than the controls, **1**, **3** and CA074. The isolated phytochemical compounds showed tight E$_b$ ranging from –5.81 to –4.51 kcal/mole to cathepsin B, compared to the controls and CA074 which ranged from -5.72 to –3.81 kcal/mole. The active site of CatB CP comprised residues of cysteine, histidine and asparagine basic nucleophilic triad which orientates the histidine and neutralizes the His charge on hydrolysis [22]. This triad, positioned between the L- and R- domains of CP, are Cys122, His282 and Asn302 from the L- and R-domains [14]. The amide group of Asn302 is supported by amine π interactions of Trp308 and Trp304 while His194 and His195 play a significant role in the enzyme's endopeptidase activity [12-14].

In the docking validation of CA074 in the deposited crystal structure complex; H-bonds between CA074 and the CatB dominated the hydrophobic interactions [13]. The H-bonds of CA074 with N atoms of Gln116 and Cys122 resulted in the stabilization of the tetrahedral intermediate of substrate hydrolysis by the oxyanion hole [22]. Information extracted from the analysis of important molecular interactions formed between potential drug compounds and protein targets is essential because it guides the derivatization of ligand in structure-activity optimization exercise. The binding modes of the **1**-**3** and the two reference compounds were determined. Docking screening of **1-3** against TbCatB protein revealed all compounds exhibiting better binding potential than the controls and CA074. Compound **2** interacted specifically with Cys119 and Cys205; **3** with Ser 117, Ala118 and Gly164, while **1** did not show any specific interaction exclusively not seen in others. All the three compounds showed a common interaction with Gly281, Cys122 and His282. The existing specific hydrophobic interaction between the cyclic ring of **1** and the –SH group of Cys122 (compared with a corresponding H-bond in **2**) could explain the specifically high *in vitro* IC$_{50}$ data against *T. congolense*. The visibly low E$_b$ (-5.81 kcal/mol) and high K$_i$ (55.21 µM) of **2** when compared with

diminazene (-5.64 kcal/mol; 73.84 μM) and CA074 (-5.72 kcal/mol; 64.45 μM) could also be attributed to the specific interaction between **2** and Cys119 and Cys205. However, the presence of Cys205 and Cys 119, in addition to the His110 and His111 of the occluding loop of Cathepsin B [23], and their interactions with the standards respectively further suggests that only interaction with Cys119 could be responsible for anti-trypanosomal activities.

CONCLUSION

Three bioactive compounds have been successfully isolated from *C. dolichopetalum*. Compound **1** is a butyl gallate, and compounds **2** and **3** are isomeric C-glycosyl flavonoids. Compound **1** exhibits strong *in vitro* activities against *T. brucei brucei* and *T. congolense* with IC$_{50}$ values of 2.72 and 0.80 μM, respectively. In addition to the interaction of **1-3**, diminazene and CA074 in the *in silico* study, additional interaction with Cys119 could be responsible for the anti-trypanosomal activities. These findings have contributed new knowledge to natural products-induced anti-trypanosomal activities by constituents of *C. dolichopetalum*.

DECLARATIONS

Conflict of interest

No conflict of interest is associated with this work.

Conference publication

This study was presented at the 2020 one-day LatinXChem Twitter conference, and the abstract published by Morressier at http://doi.org.10.26226/morressier.5f6c5f439b74b699bf390b50.

Contribution of authors

We declare that this work was done by the authors named in this manuscript and all liabilities on claims relating to the content of this article will be borne by the authors. All the authors contributed equally in the conceptualization, design, bench work, documentation, data analyses and manuscript preparation.

REFERENCES

1. *Muhanguzi D, Mugenyi A, Bigirwa G, Kamusiime M, Kitibwa A, Akurut GG, Ochwo S, Amanyire W, Okech SG, Hattendorf J, et al. African animal trypanosomiasis as a constraint to livestock health and production in Karamoja region: A detailed qualitative and quantitative assessment. BMC Vet Res 2017; 13(1): 1-13. https://doi.org/10.1186/s12917-017-1285-z.*

2. *Meyer A, Holt HR, Selby R, Guitian J. Past and ongoing tsetse and animal trypanosomiasis control operations in five African countries: A systematic review. PLoS Negl Trop Dis 2016; 10(12): e0005247. https://doi.org/10.1371/journal.pntd.0005247.*

3. *Nnadi CO, Nwodo NJ, Kaiser M, Brun R, Schmidt TJ. Steroid alkaloids from Holarrhena africana with strong activity against Trypanosoma brucei rhodesiense. Molecules 2017; 22(7): 1129*

4. *Pereira SS, de Almeida Neto KJDAC, Duffy CW, Richards P, Noyes H, Ogugo M, André MR, Bengaly Z, Kemp S, Teixeira MM, et al. Variant antigen diversity in Trypanosoma vivax is not driven by recombination. Natur Comm 2020; 11(1): 1-13. https://doi.org/10.1101/733998.*

5. *Giordani F, Morrison LJ, Rowan TG, De Koning HP, Barrett MP. The animal trypanosomiases and their chemotherapy: A review. Parasitol 2016; 143(14): 1862-1889. https://doi.org/10.1017/S0031182016001268.*

6. *Nnadi CO, Althaus JB, Nwodo NJ, Schmidt TJ. A 3D-QSAR study on the anti-trypanosomal and cytotoxic activities of steroid alkaloids by comparative molecular field analysis. Molecules 2018; 23(5): 1113.*

7. *Nnadi CO, Ngwu SO, Ohagwu MBZ. In vivo and in silico evidence of anti-trypanosomal activities of selected plants from Asteraceae family against Trypanosoma brucei brucei. Bioint Res Appl Chem 2023; 13(1): 1-10. https://doi.org/10.33263/BRIAC131.030.*

8. *Hoet S, Opperdoes F, Brun R, Quetin-Leclercq J. Natural products active against African trypanosomes: A step towards new drugs. Nat Prod Rep 2004; 21(3): 353-364. https://doi.org/10.1039/b311021b.*

9. Asuzu IU, Onu OU. Anti-ulcer activity of the ethanolic extract of Combretum dolichopetalum root. J Pharm Biol 1990; 28: 27-32. https://doi.org/10.3109/13880 209009082770.

10. Udem SC, Madubunyi I, Asuzu IU, Anika SM. The trypanocidal action of the root extract of Combretum dolichopetalum. Fitoter 1996; 67: 31-37.

11. Gugu TH, Eze CO, Kenechukwu FC, Nnadi CO, Ofokansi KC, Attama AA, Esimone CO. In vitro and in vivo biological evaluations of Combretum dolichopetalum leave extract and fractions in the management of some tropical diseases. IOSR J Pharm Biol Sci 2019; 14(1): 47-60. http://doi.org/10.9790/3008-1401044760.

12. Kerr ID, Wu P, Marion-Tsukamaki R, Mackey ZB, Brinen LS. Crystal structures of TbCatB and rhodesain, potential chemotherapeutic targets and major cysteine proteases of Trypanosoma brucei. PLoS Negl Trop Dis 2010; 4(6): e701. https://doi.org/10.1371/journal. pntd.0000701.

13. Redecke L, Nass K, DePonte DP, White TA, Rehders D, Barty A, Stellato F, Liang M, Barends TRM, Boutet S, et al. Natively inhibited Trypanosoma brucei Cathepsin B structure determined by using an X-ray laser. Sci 2013; 11, 339(6116): 227–230. https://doi.org/10.1126/ science. 1229663.

14. Unciti-Broceta JD, Maceira J, Morales S, García-Pérez A, Muñóz-Torres ME, Garcia-Salcedo JA. Nicotinamide inhibits the lysosomal Cathepsin b-like protease and kills African trypanosomes. J Biol Chem 2013; 288(15): 10548–10557. https://doi.org/10.1074/jbc.m112.449207.

15. Nnadi CO, Ebiloma GU, Black JA, Nwodo NJ, Lemgruber L, Schmidt TJ, de Koning HP. Potent anti-trypanosomal activities of 3-aminosteroids against African trypanosomes: Investigation of cellular effects and of cross-resistance with existing drugs. Molecules 2019; 24(1): 268. https://dx.doi.org/10.3390%2Fmolecules 24020268.

16. Berman HM, Westbrook J, Feng Z, Gilliland G, Bhat TN, Weissig H, Shindyalov I.N, Bourne PE. The Protein Data Bank. Nucleic Acids Res 2000; 28(1): 235–242. https://doi.org/10.1093/nar/28.1.235.

17. Ibezim A, Onuku RS, Ibezim A, Ntie-Kang F, Nwodo NJ, Adikwu MU. Structure-based virtual screening and molecular dynamics simulation studies to discover new SARS-CoV-2 main protease inhibitors, Sci Afr 2021; 14: e00970. https://doi.org/10.1016/j.sciaf.2021.e00970.

18. Trott O, Olson AJ. AutoDock Vina: Improving the speed and accuracy of docking with a new scoring function, efficient optimization, and multithreading. J Comput Chem 2010; 31(2): 455–461. https://dx.doi.org/10. 1002%2Fjcc.21334.

19. Yu XX, Huang JY, Xu D, Xie ZY, Xie ZS, Xu XJ. Isolation and purification of orientin and vitexin from Trollius chinensis Bunge by high-speed counter-current chromatography. Nat Prod Res 2014; 28(9): 674-676. https://doi.org/10.1080/14786419.2014.891111.

20. Kharas GB, Spann T, Dawood R, Malik S, Deleon IJ, Estes MA, Gilbert JM, Goshu BA, Harris ED, Kyoseva TD, et al. Novel copolymers of styrene. 1. Alkyl ring-substituted butyl 2-cyano-3-phenyl-2-propenoates. J Macromol Sci Part A 2015; 52(7): 499-503. https://doi.org/10.1080/10601325.2015.1039317.

21. Latté KP, Kaloga M, Schäfer A, Kolodziej H. An ellagitannin, n-butyl gallate, two aryltetralin lignans and an unprecedented diterpene ester from Pelargonium reniforme. Phytochem 2008; 69(3): 820-826. https://doi.org/10.1016/j.phytochem.2007.08.032

22. Rzychon M, Chmiel D, Stec-Niemczyk J. Modes of inhibition of cysteine proteases. Acta Biochim Pol 2004; 51(4): 861–873.

23. Mendoza-Palomares C, Biteau N, Giroud C, Coustou V, Coetzer T, Authie´ E, Boulange´ A, Baltz T. Molecular and biochemical characterization of a Cathepsin B-like protease family unique to Trypanosoma congolense. Eukary Cell 2008; 7(4): 684–697. https://doi.org/10.1128/EC.00405-07.